A statistical approach to determining the uncertainty of peat thickness

J. Torppa

Eastern Finland Office, Geological Survey of Finland

SUMMARY

This paper presents statistical studies of peat thickness to define its expected maximum variation ($\Delta d_m(\Delta r)$) as a function of separation distance Δr. The aim was to provide an estimate of the observational uncertainty in peat depth due to positioning error, and the prediction uncertainty of the computed model. The data were GPS position and ground penetrating radar depth measurements of six mires in different parts of Finland. The calculated observational uncertainty for Finnish mires in general caused, for example, by a 20 m positioning error, is 43 cm in depth with 95 % confidence. The peat depth statistics differed among the six mires, and it is recommended that the mire specific function $\Delta d_m(\Delta r)$ is defined for each individual mire to obtain the best estimate of observational uncertainty. Knowledge of the observational error and function $\Delta d_m(\Delta r)$ should be used in peat depth modelling for defining the uncertainty of depth predictions.

KEY WORDS: depth, mathematics, mire, modelling, observations, statistics.

INTRODUCTON

To draw reliable conclusions from any data, its uncertainty should be considered. In geological observations and modelling, however, uncertainty is mostly hard to define quantitatively, and it is often disregarded. This is also the case in peat depth studies. The topography of the Finnish Precambrian bedrock varies, and was modified by the recent ice age. The result is that steep slopes and large erratic boulders appear at the bases of peat profiles. The unpredictable spatial alteration of peat thickness makes 3D modelling of peatlands demanding, and estimates of prediction uncertainty are not usually given with the depth predictions. Uncertainty is, however, an essential part of any model.

Peat thickness data have several sources of error, depending on the method of observation. In coring data, there is error due to the fuzzy upper boundary of the peat layer, roughness of the surface, reading accuracy, and the positioning error. In ground penetrating radar (GPR) data there is measurement error caused by imperfections of the instrument, error in interpretation of the data, and error due to inaccurate positioning. Aerogeophysical data error has a number of sources, many of which are hard to define (Suppala 2010, personal communication). Thorough reviews of how to consider uncertainty in geology, quantitatively or qualitatively, are given by Bárdossy & Fodor (2001) and by Gustavsson (2010).

Coring observations are the main source of information on peat thickness in peatland studies carried out by the Geological Survey of Finland (GTK). The depth values are read from the core drill with 10 cm accuracy, causing a 5 cm uncertainty. The effect of the fuzzy upper limit of the peat layer is negligible compared to the reading error (Jukka Turunen, personal communication). This article is concerned with the third source of error, i.e., that caused by the positioning error, which depends on the spatial variations of peat depth. The spatial statistics of peat thickness can be studied only by using closely spaced depth measurements. Technical development of the GPR measurement systems now allows us to obtain high spatial resolution measurements of peat depths from various types of mire. The GPR equipments use radar to measure depth and GPS to measure position. The snake-like rough-terrain-antenna GPR system, that was purchased for the GTK in 2009, is transportable over even densely ditched mires and in thickets, and a systematic grid of measurements can be collected throughout any mire that can be walked over. The GPR measuring system and its use in peat research are described by Leino (2010).

In this article the dense GPR data were used to define the expected maximum variation of peat thickness, ($\Delta d_m(\Delta r)$) as a function of distance, Δr, and this in turn was used to determine the uncertainty of peat thickness observations and the prediction uncertainty of interpolated depth values. This work was part of the peatland inventory method project, started at GTK in 2009, which aims to develop more efficient observational methods and more accurate modelling of peat thickness and properties.

TEST DATA AND METHODS

GPR measurements on six mires were used. On three (Heinäsuo, Koivulamminneva and Pikarineva), GPR measurements were made using MALÅ Geoscience's Ramac with a 100 MHz rough terrain antenna. On Länkkyjärvenneva the GPR equipment was GSSI's SIR-3000 with a 200 MHz antenna. On Kakkurisuo and Mustaneva the GPR equipment was GSSI's SIR-3000 with a 100 MHz antenna.

The GPR signal was practically continuous for the path the measuring system was transported along. The peat depth was interpreted at specific locations along the path using the Roadscanners' GeoDoctor 2 program. The data are summarised in Table 1 and the locations of the interpreted points on each mire are shown in Figures 1–7. From Heinäsuo there are two datasets; one with lower and the other with higher spatial resolution. Three of the datasets (Heinäsuo1, Koivulamminneva and Länkkyjärvenneva) cover the major part of the peatland area while the rest (Heinäsuo2, Pikarineva, Kakkurisuo and Mustaneva) cover only a small part of the mire.

Peat depth statistics

To be able to define the uncertainty of an observation due to positioning error, and the uncertainty of interpolated model depths, one must study statistically the spatial variations of peat thickness. Examples of how the peat depth difference changes as a function of separation distance are shown with two semivariogram clouds derived from our dataset in Figures 8 and 9. In geostatistics, a semivariogram cloud of a sample of a quantity defined, for instance, in space or time is a plot of the half squared difference between the values of each pair of sample points as a function of distance or time difference between the points. Our sample consists of peat depth measurements at specific locations, and the semivariance and separation distance (γ_{ij} , Δr_{ij}) defining the semi-variogram cloud are:

$$\gamma_{ij} = \frac{1}{2}(d_i - d_j)^2 \qquad [1]$$

$$\Delta r = \sqrt{(x_i - x_j)^2 + (y_i - y_j)^2} \qquad [2]$$

where d_i and d_j are the depths of the sample points i and j, and x_i,y_i and x_j,y_j are their geographical locations.

Table 1. Summary of the data. N is the number of data points, Δ is the separation between subsequent interpretations on the GPR observation line, MinD, MaxD and MeanD are the minimum, maximum and mean interpreted depths, and σD is the standard deviation of the depth.

Mire name/ dataset	N	Δ (m)	Mire base	Location	MinD (cm)	MaxD (cm)	MeanD (cm)	σD (cm)
Heinäsuo1 [1,2]	463	20		Valtimo	0	440	166	114
Heinäsuo2 [1,2]	779	1		Valtimo	0	392	139	133
Heinäsuo1+2 [1,2]	1242	1–20	57% silt 30 % moraine 13% others	Valtimo	0	440	149	127
Koivulamminneva [1]	384	10–20	65 % moraine 18 % sand 10 % silt	Kivijärvi	1	435	188	118
Pikarineva [2]	129	15–20	57% moraine 20% sand 10 % clay 7 % fine sand	Rantsila	18	196	127	45
Länkkyjärvenneva [3]	1247	10–50	?	Kruunupyy	20	440	151	66
Kakkurisuo [4]	536	1	clay	Köyliö	5	415	291	98
Mustaneva [4]	402	1	clay	Lavia	428	533	482	28
Combined dataset					0	533	206	142

Data provided by: [1] Matti Laatikainen (GTK) , [2] Jukka Leino (GTK), [3] Ahlholmens Kraft Oy, Miikka Paalijärvi (GTK), [4] Timo Suomi (GTK).

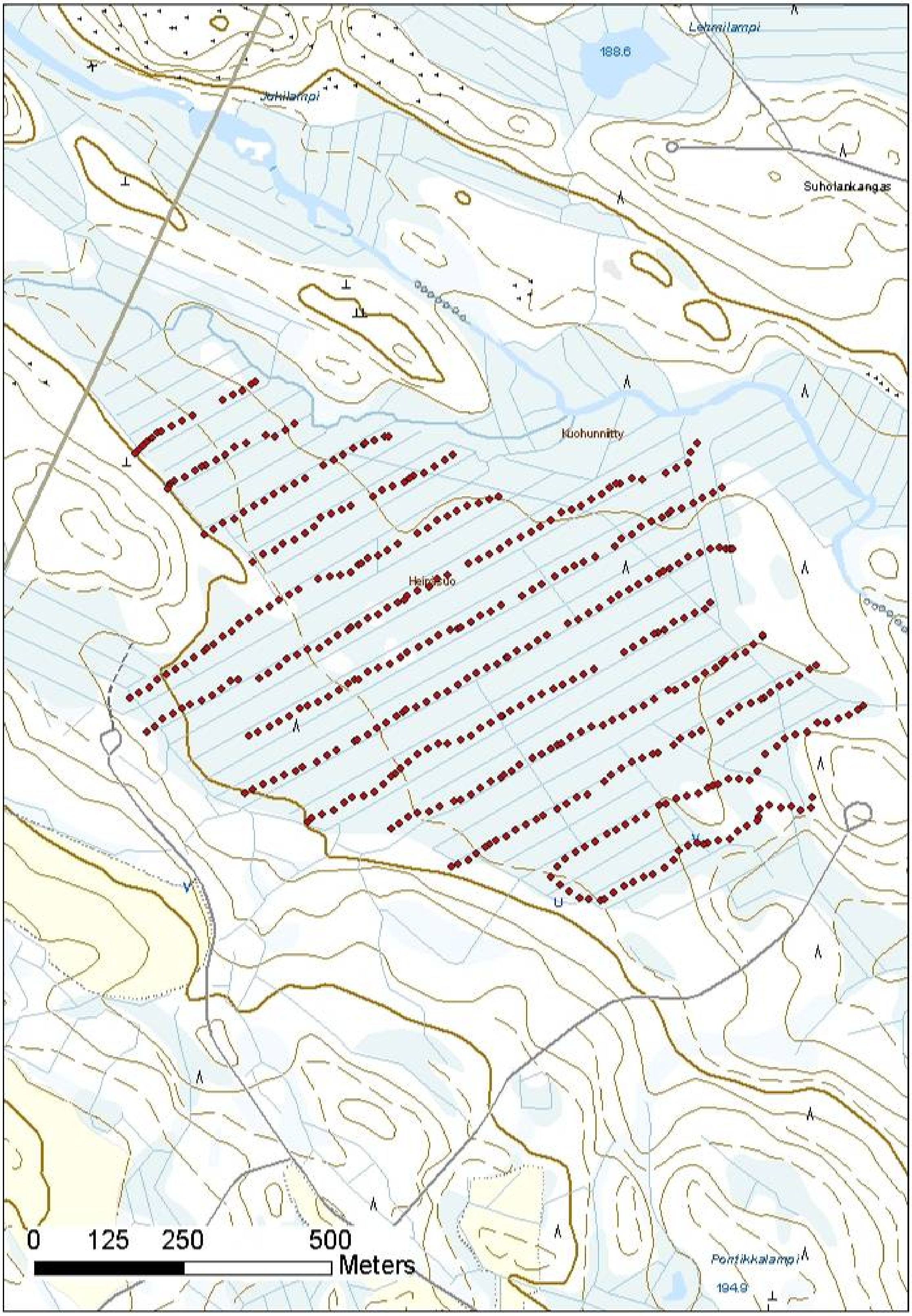

Figure 1. Map of Heinäsuo showing the GPR (ground penetrating radar) interpretation locations as black diamonds with red filling. Dataset Heinäsuo1. Brown curves: 5 m elevation contours (continuous), 2.5 m elevation contours (dashed); light blue areas: mires; darker blue features: lakes, streams and ditches (on peat); thin curved grey lines: small roads; thicker grey lines: municipality borders.

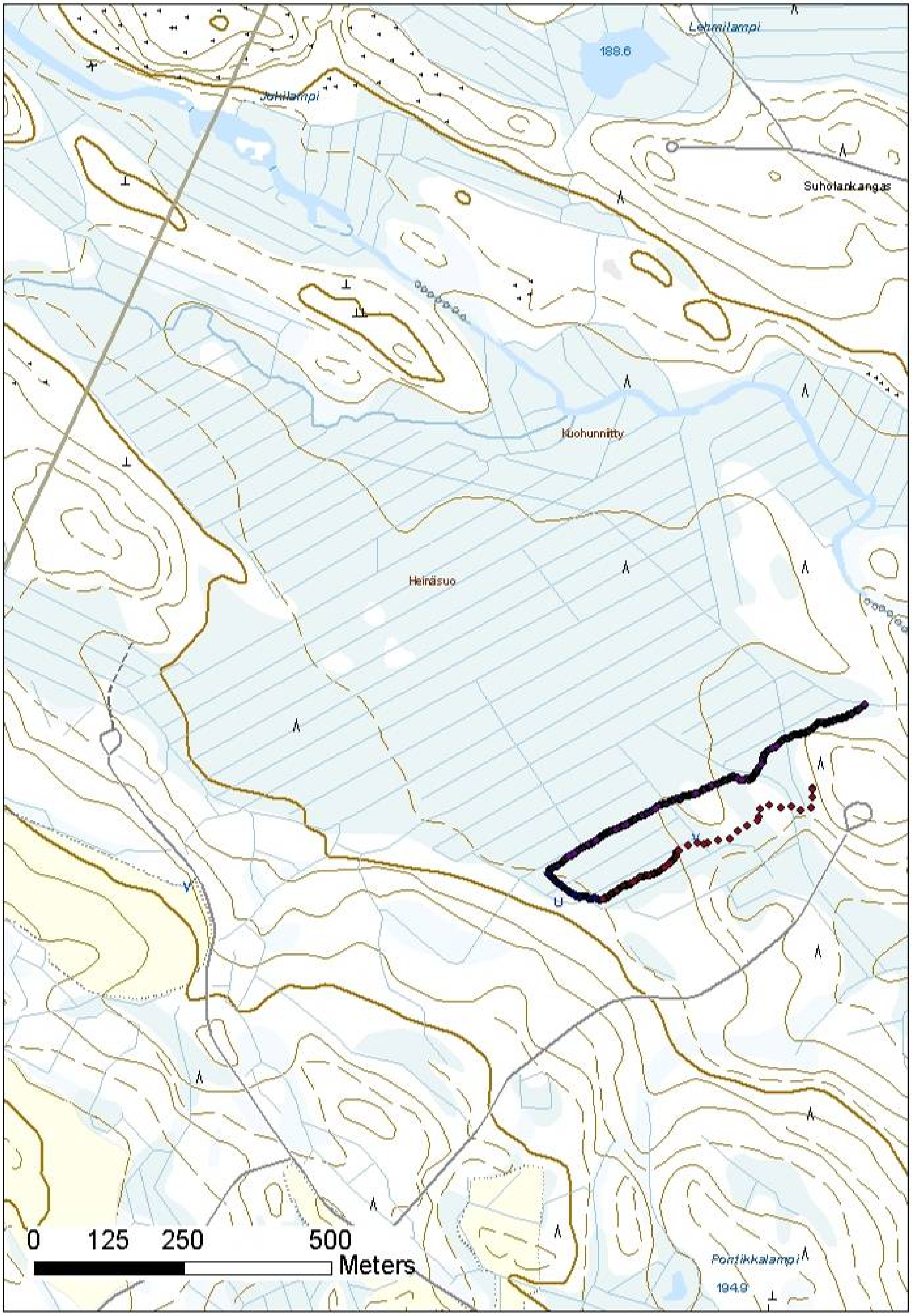

Figure 2. Map of Heinäsuo showing the GPR (ground penetrating radar) interpretation locations as colour-filled black diamonds. Dataset Heinäsuo2. For cartographic explanations, see Figure 1.

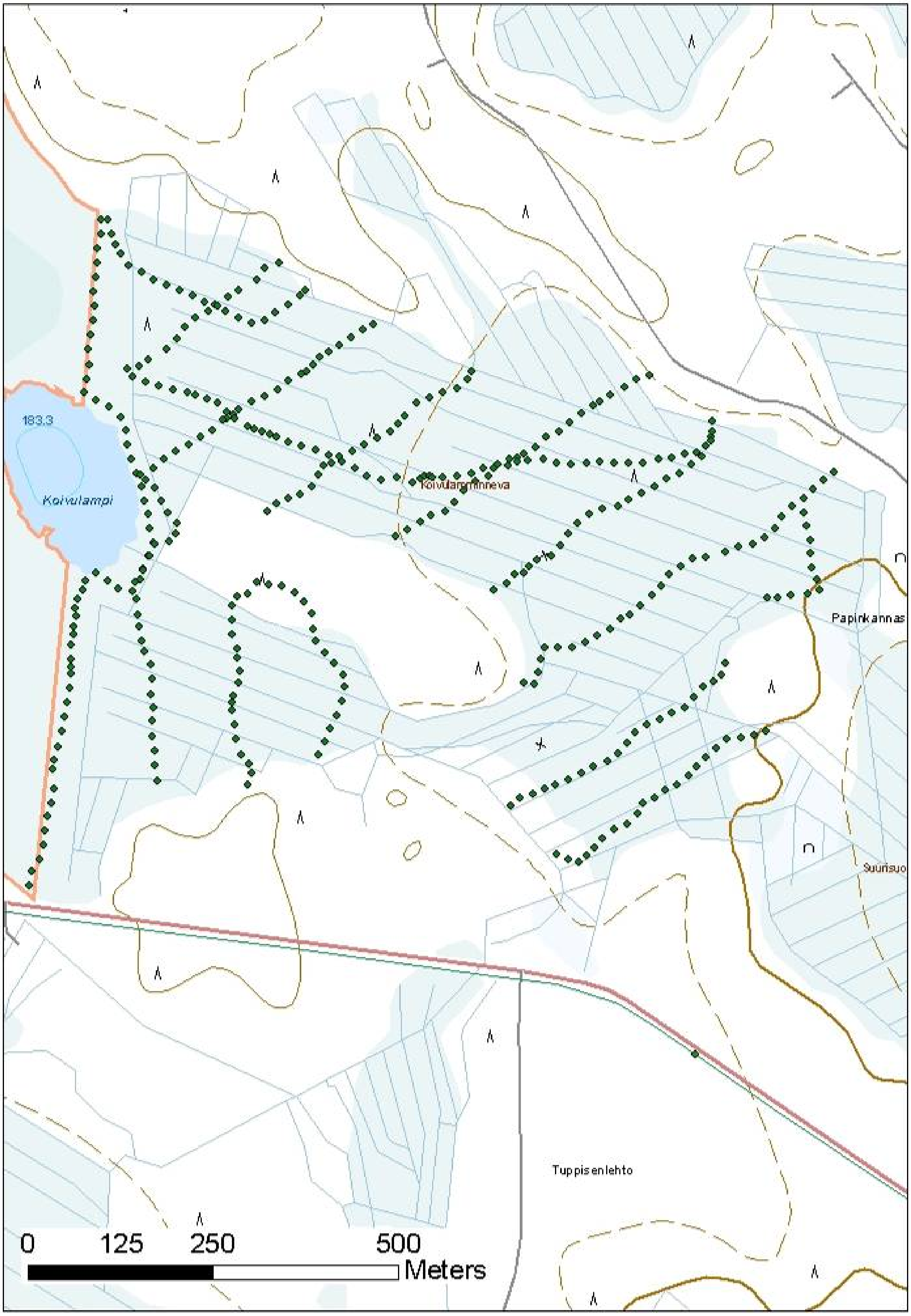

Figure 3. Map of Koivulamminneva showing the GPR interpretation locations as black diamonds with green filling. Green lines are electricity power lines. For other cartographic explanations, see Figure 1.

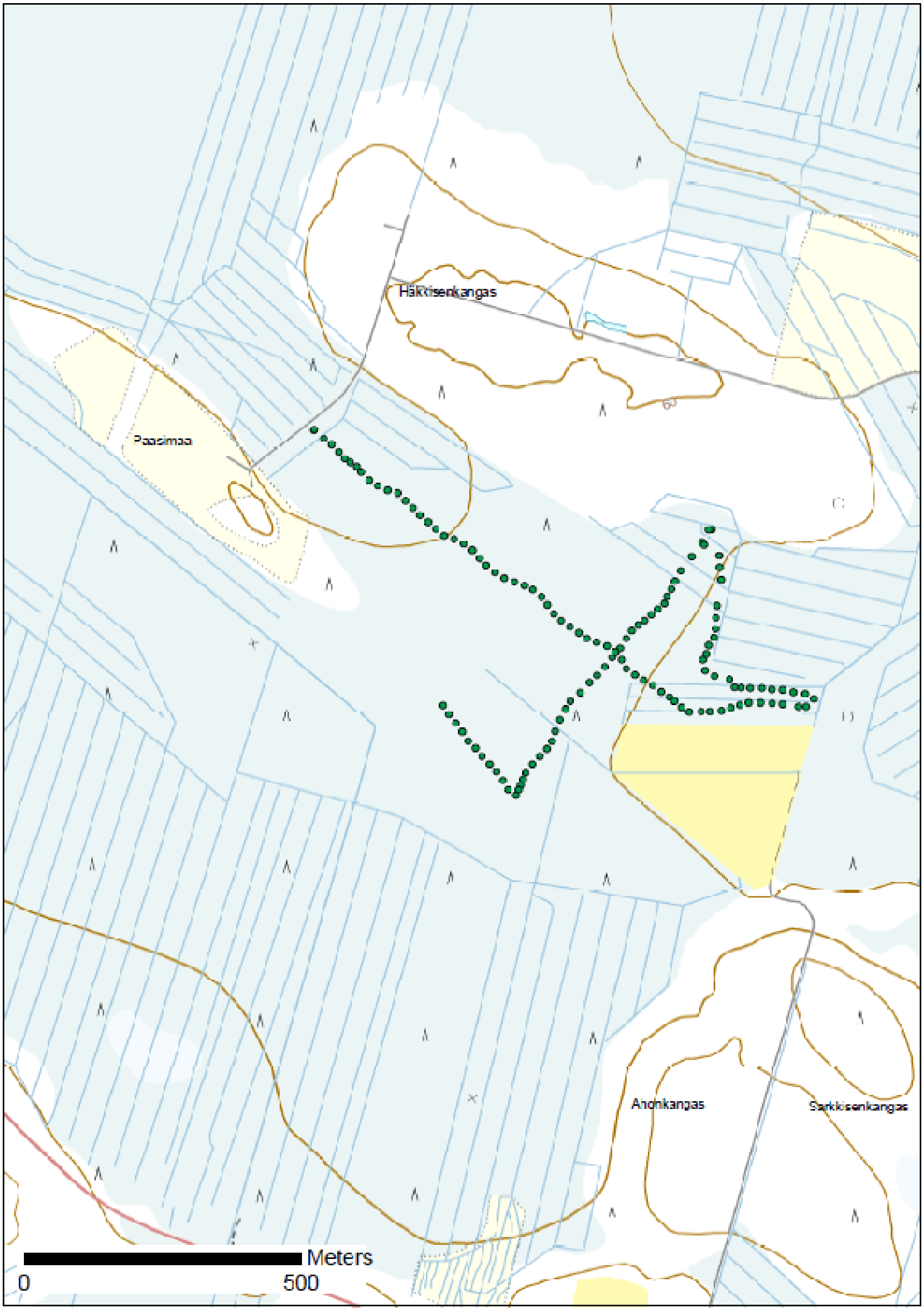

Figure 4. Map of Pikarineva showing the GPR interpretation locations as black circles with cyan filling. Yellow areas are fields. For other cartographic explanations, see Figure 1.

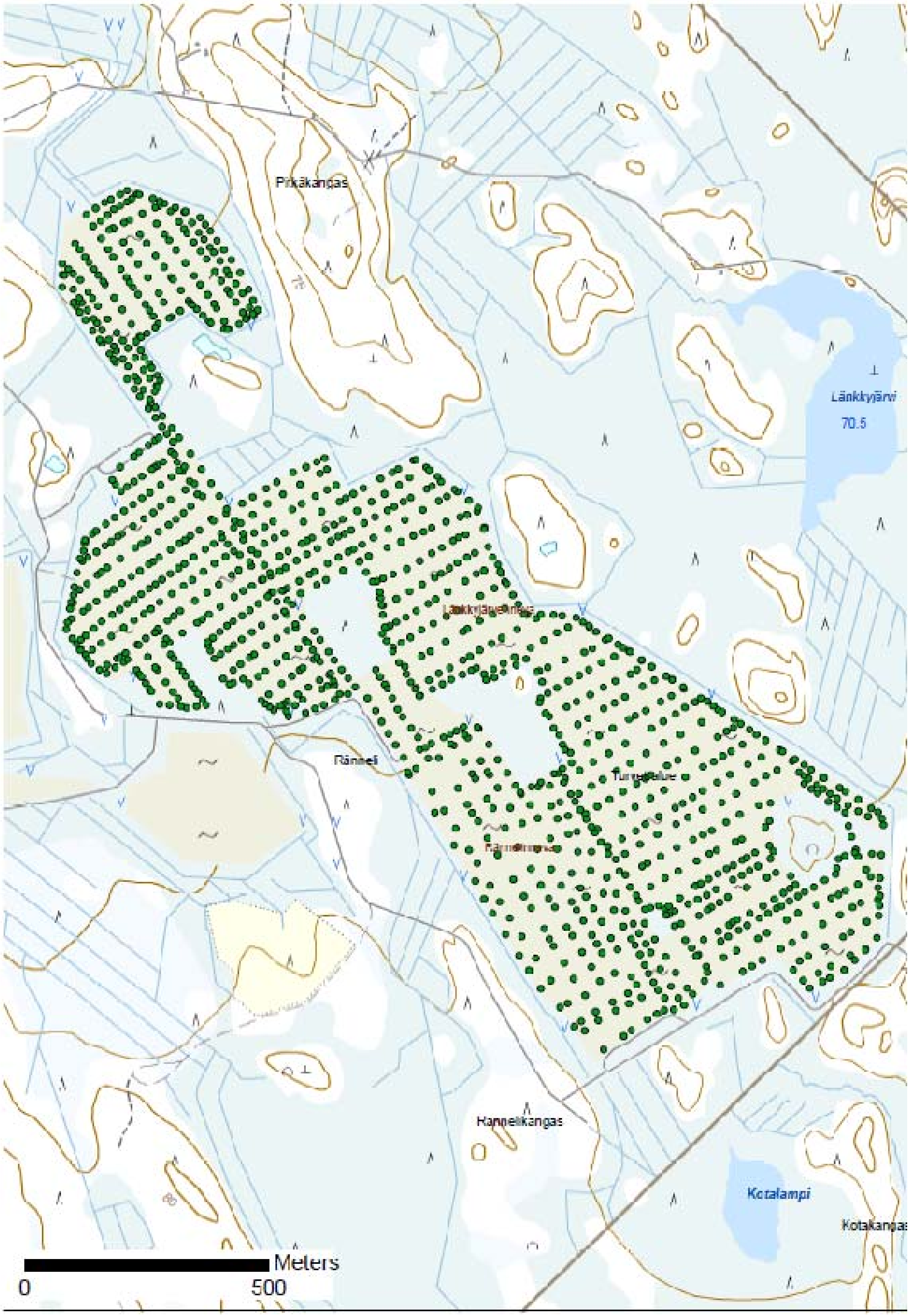

Figure 5. Map of Länkkyjärvenneva showing the GPR interpretation locations as black circles with green filling. The brownish-grey colour of the study area represents a peat production area. For other cartographic explanations, see Figure 1.

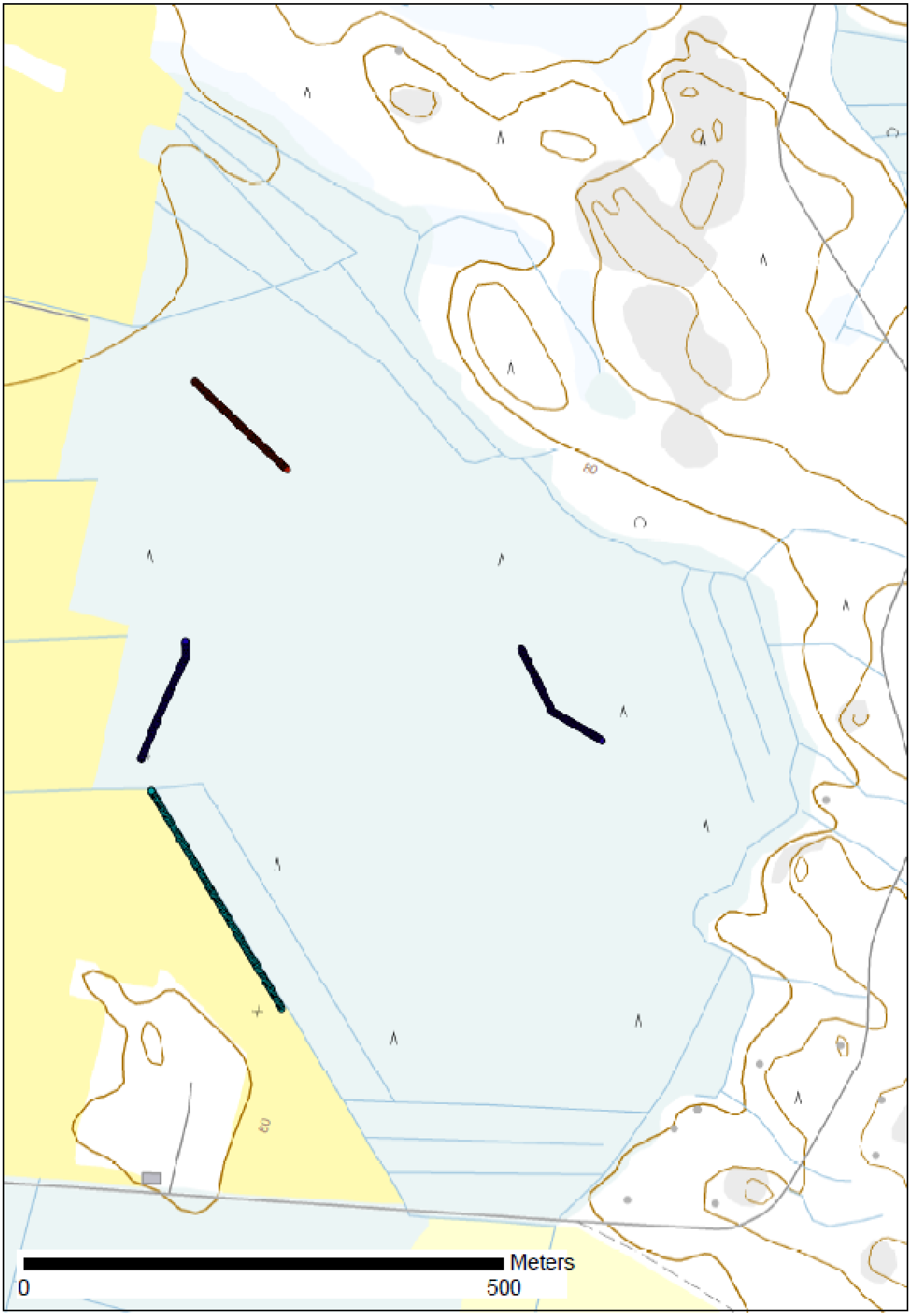

Figure 6. Map of Kakkurisuo showing the GPR interpretation locations as colour-filled black circles. Yellow areas are fields. For other cartographic explanations, see Figure 1.

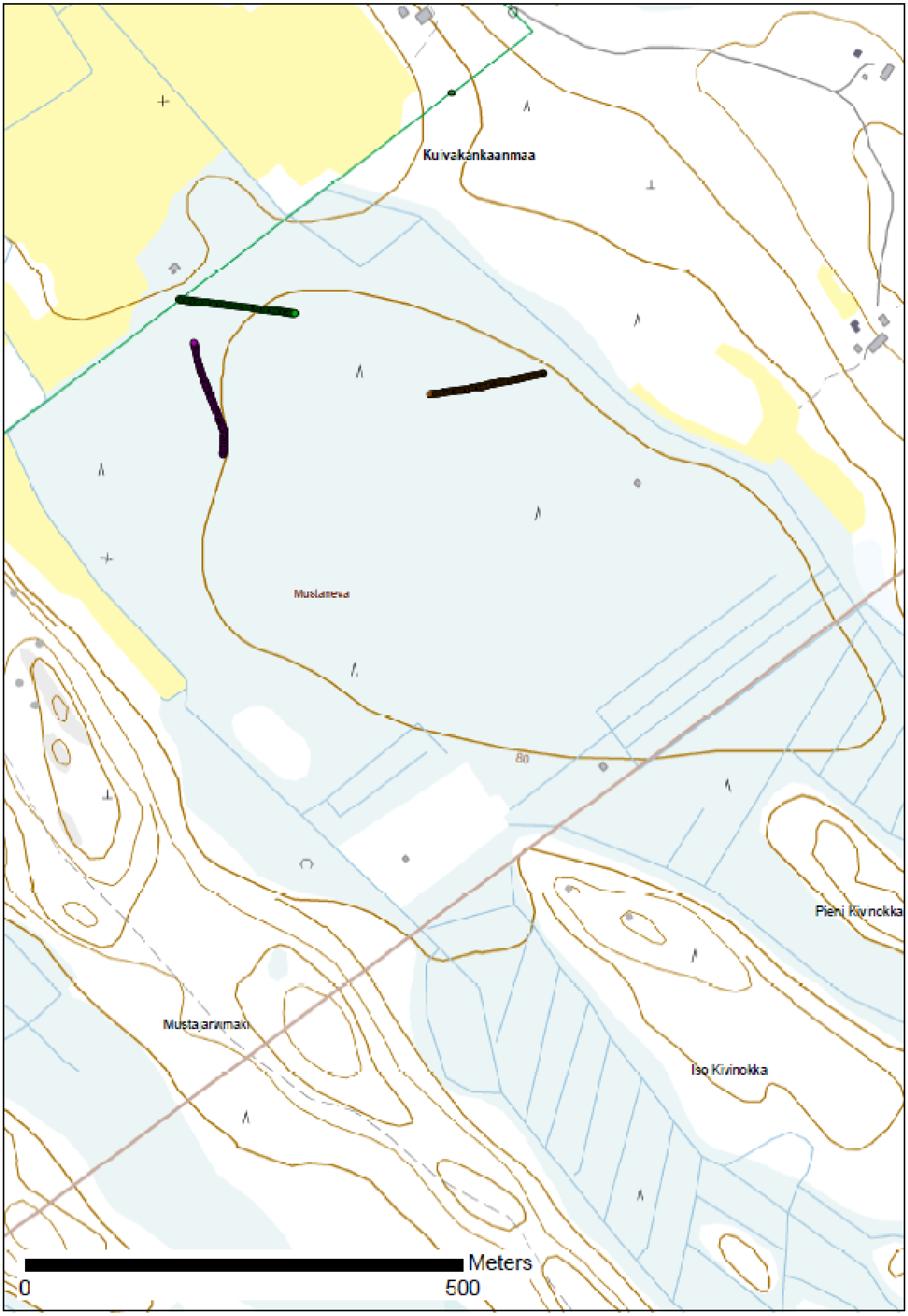

Figure 7. Map of Mustaneva showing the GPR interpretation locations as colour-filled black circles. Green lines are electricity power lines and yellow areas are fields. For other cartographic explanations, see Figure 1.

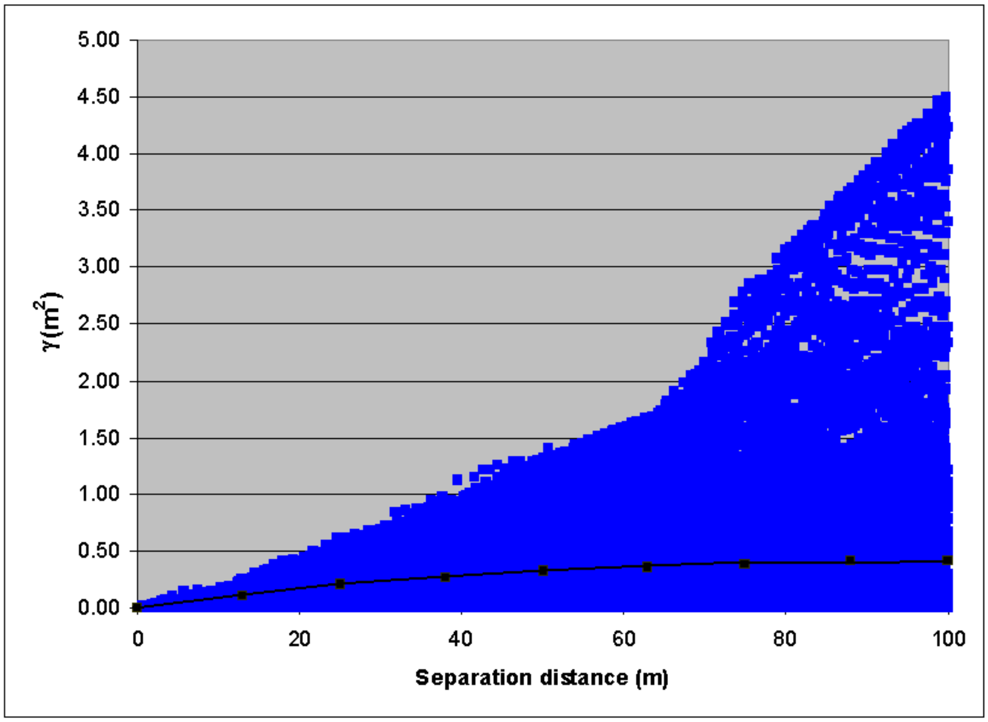

Figure 8. Semivariogram cloud of the Heinäsuo2 data for separation distance range 0–100m. Each blue square is one of the pairwise comparisons of GPR depth data, and the black line is the fitted exponential semivariogram function. The quantity on the *y*-axis is $\gamma=0.5*(d_i-d_j)^2$, where d_i and d_j are peat depths at any two different GPR data points *i* and *j*. The distance on *x*-axis is the distance between data points *i* and *j*.

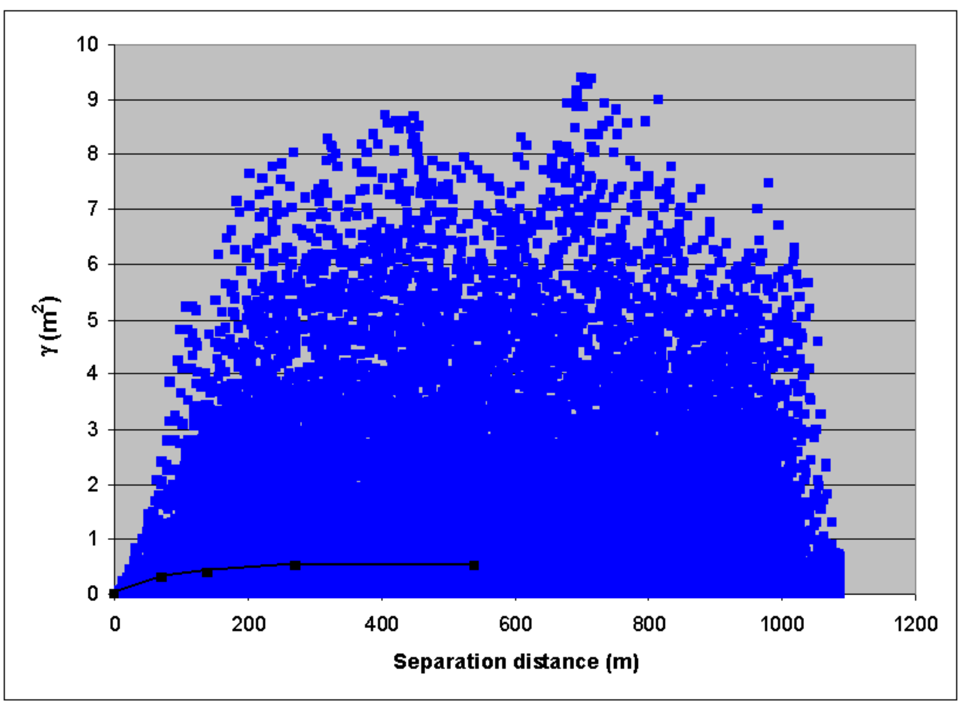

Figure 9. Semivariogram cloud of the Koivulamminneva data for separation distance range 0–1100 m. Each blue square is one of the pairwise comparisons of GPR depth data and the black line is the fitted exponential semivariogram function. The quantity on *y*-axis is $\gamma=0.5*(d_i-d_j)^2$, where d_i and d_j are peat depths at any two different GPR data points *i* and *j*. The distance on *x*-axis is the distance between data points *i* and *j*.

The semivariogram clouds in Figures 8 and 9 are computed for distance ranges 100 m (Heinäsuo2) and 1100 m (Koivulamminneva, entire dataset). The semivariance on the y-axis is given in m^2 and the separation distance in metres.

The Heinäsuo2 data (Figure 8) represent a case where interpretations have been carried out with high spatial density (1 point/m) producing a semivariogram cloud clearly showing how the characteristic maximum depth difference increases with increasing separation distance at distances less than 100 m. Such spatially dense data are expensive to generate and, thus, not expected to be generally available in the near future. However, it is important to have such data from a few peatlands to get an idea of how the peat depth changes at small separation distances on different types of mires. The fitted exponential semivariogram is strongly dominated by the small depth differences.

The data from Koivulamminneva (Figure 9) have a more typical interpretation density of (1 point/10–20m). This is not dense enough to generate a representative semivariogram cloud for small distances, but sufficient to generally describe the change of the maximum depth difference as a function of separation distance. Since the data cover the entire peatland, the semivariogram cloud shows clearly how the maximum depth difference first increases with increasing separation distance, and then reaches a constant value at a separation distance of 100 m. The fitted exponential-linear semivariogram is, again, dominated by the small depth differences.

In the above examples, the semivariogram was fitted to the mean values of the depth differences in each lag of separation distance, which is a common habit in geostatistics. (A lag means one section of discretised separation distance, when depth differences are divided into groups with similar separation distances). It is evident that the semivariogram is strongly dominated by small depth differences, which are much more frequent than larger differences at all separation distances. In fact, the distribution of depth differences in each lag is not Gaussian but half-Gaussian with zero mean, which means that the mean value of the variable is not its expectation value. Figure 10 shows, as an example, the frequency distributions of depth differences for a set of separation distance lags for the entire dataset. (Semivariances are not considered from now on, since we are interested in the depth difference itself, not the semivariance of the depth.) Also shown, in Figure 10, are example fits of half-Gaussian distributions with zero mean; one to the range 0–5 m, one to the range 50–105 m (Figure 10a) and a third one to the range of 150–455 m (Figure 10b) separation distances.

In this study, the half-Gaussian distribution was fitted to the data to obtain function $\Delta d_m(\Delta r)$, i.e. the depth difference at separation distance Δr below which the observed depth differences lie with a certain probability. We want to reach the level of 95 % confidence, corresponding to 2σ of a Gaussian distribution. The necessary statistic function $\Delta d_m(\Delta r)$ is obtained from a set of observed peat depths:

1) compute the depth difference between each pair of observed points ($\Delta d_{ij} = |d_i - d_j|$);
2) compute the separation distance between each pair of observed points ($\Delta r_{ij} = |r_i - r_j|$);
3) divide range Δr_{ij} into sections of equal width (lags);
4) fit a Gaussian distribution to the depth difference frequencies in each lag;
5) calculate Δd_m (=2σ of the fitted Gaussian distribution) for each lag; then
6) fit the function $\Delta d_m(\Delta r)$ to the set of $(\Delta d_m, \Delta r_{ij})$ values.

The last step is carried out here using either an exponential function commonly fitted to empirical semivariogram clouds

$$\Delta d_m(\Delta r) = D_0 + w\left(1 - e^{-\frac{\Delta r}{a}}\right) \qquad [3]$$

or a linear function

$$\Delta d_m(\Delta r) = D_0 + k\Delta r \qquad [4]$$

where D_0, w, a and k are four free parameters. The fitted models and parameters are purely mathematical, i.e. they have no physical basis. Dimensions of the parameters are: $[D_0] = [w] = [a] = [\Delta d_m]$. Parameter k is dimensionless.

Since the study is based on GPR data, its uncertainty has to be considered as well. Instrument error is minimal, but interpretation and positioning cause random error in the data. The signal obtained along the track of GPR is in practice continuous, and the depth can be interpreted at any point on the track. The quantity required for interpreting the data is the dimensionless quantity called dielectric constant (ε_r) of the material. The vertical mean ε_r of the peat layer at a certain location is obtained using measured reference peat depths and the corresponding two-way light times of the GPR signal (i.e. the time it takes for the GPR signal to leave the transmitter, go to the target and come back to the receiver). The dielectric coefficient of peat is mostly affected by its water content and changes from place to place within the area of the peatland. According to a large number of dielectric coefficient

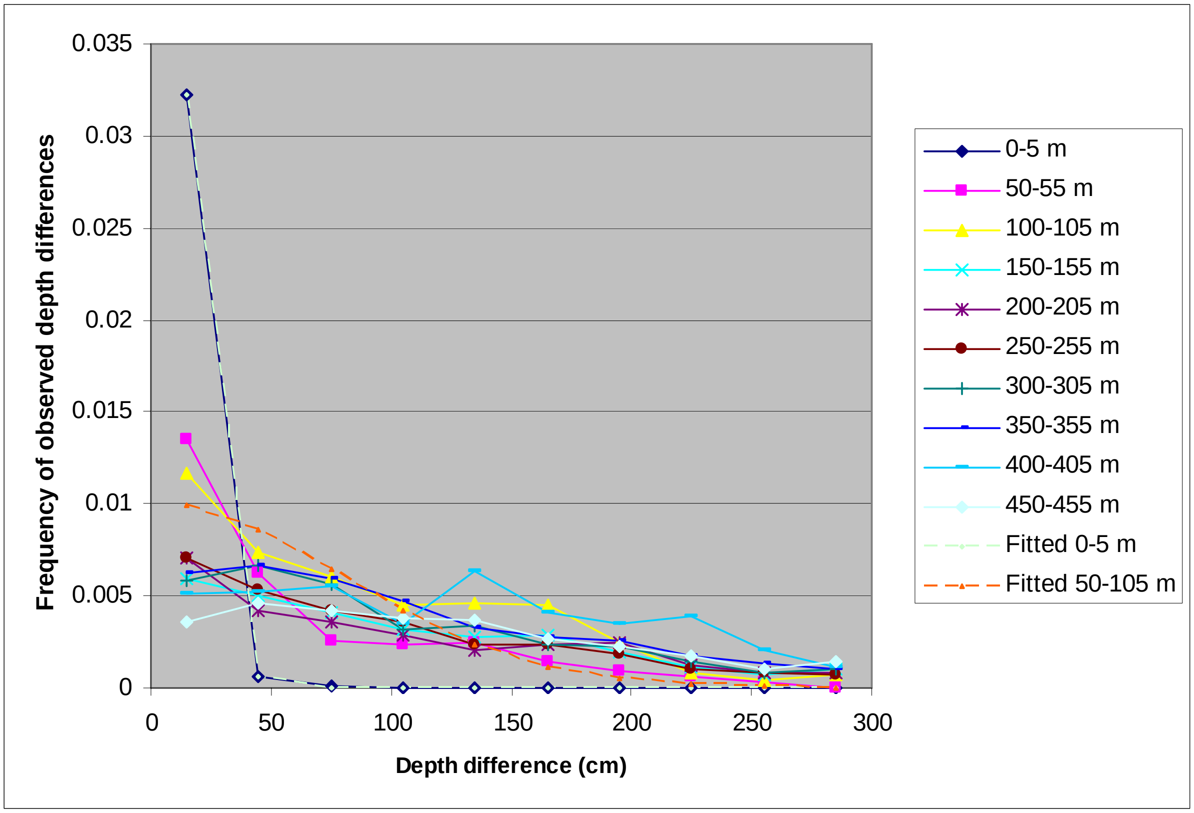

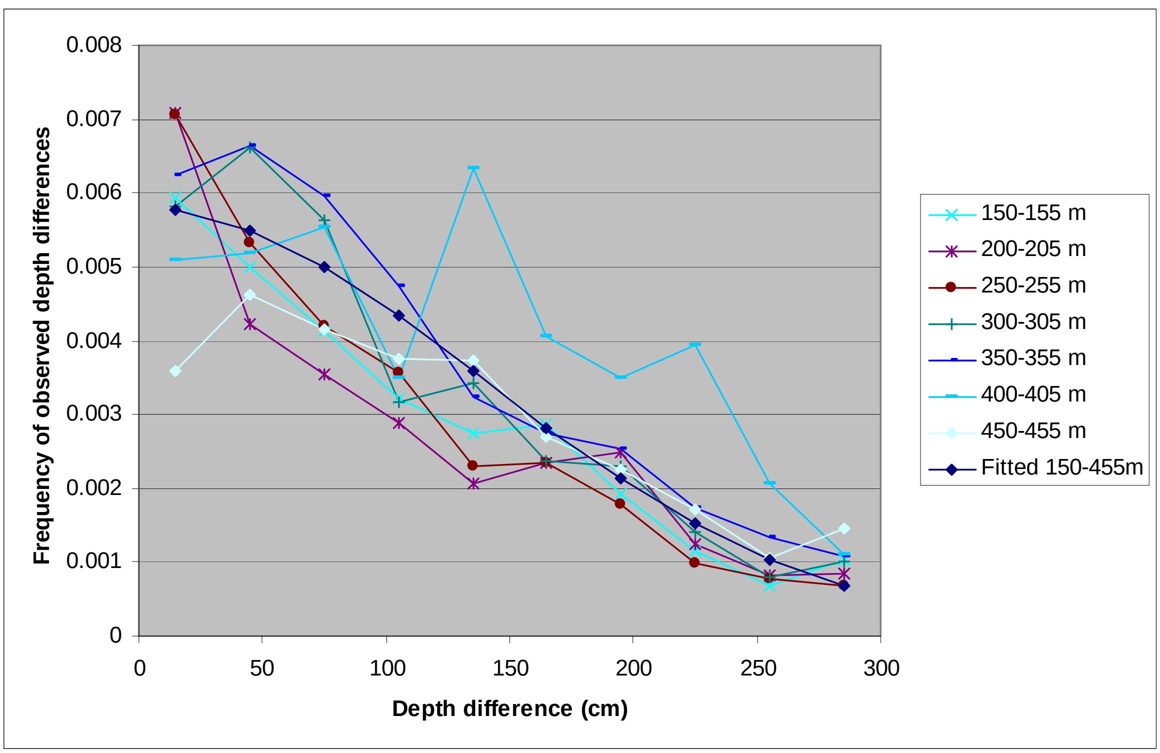

Figure 10. Normalised distributions of peat depth difference frequency for (a) ten 5 m wide separation distance lags in the range 0–455 m with Gaussian distributions fitted to 0–5 m lag and 50–55 m + 100–105 m lag data (upper diagram); and (b) eight 5 m wide separation distance lags in the range 150–455 m with the Gaussian distribution fitted to all the data points shown in the plot (lower diagram).

measurements and reference peat depth corings carried out at GTK, the range of mean ε_r for a single depth profile, with 95 % confidence, is 50–70 which corresponds to 12 % variation in peat depth for a constant two-way light time.

GPR data uncertainty must be taken into account in peat depth modelling but, due to its random nature, is not included in this study, since random error in depth values does not affect the distribution of depth differences (if the number of observed depths is sufficiently large).

Peat depth model

Kriging, which is commonly used in modelling based on geostatistics, is not appropriate for this problem because the expectation value of the semivariance of the depth is zero (see the half-Gaussian distributions in Figure 10), making it impossible to find a unique solution to the kriging equations. The depth models were computed using the MITTI modelling tool described in Torppa *et al*. (2010), modified by using function $\Delta d_m(\Delta r)$ in the uncertainty calculation. The MITTI tool was developed to take advantage of various different types of datasets in peat thickness modelling such as aerogeophysical, GPR and coring data as well as the mire outline. Part of the data consist of sparse observations while other parts may be densely observed, and each dataset has its characteristic observational error. Also, some typical geological features are taken into account in modelling. The tool is based on interpolation with parameters and weighting functions developed to be suitable for the peat depth data. The model depth values d_i are interpolated from the closest observed depth values using the standard interpolation formula

$$d_i = \sum \lambda_{ik} D_k \qquad [5]$$

where D_k is the observed depth at point k, and λ_{ik} the corresponding normalised weight for modelled point i, which decreases exponentially with increasing separation distance. Thus, the interpolation method is based on inverse distance weighting.

The interpolation method itself does not offer any estimate of the uncertainty of the model and, thus, a custom method for error estimation must be developed. To clarify how function $\Delta d_m(\Delta r)$ is used to define prediction uncertainty here, Figure 11 shows how the $\Delta d_m(\Delta r)$ part of the uncertainty can ideally be obtained midway between two observed points, 280 m apart. It is evident that if observations represent the same depth (Figure 11a) the uncertainty is larger than if different depths have been observed (Figure 11b). Following the idea represented in Figure 11, the uncertainty ε_i for prediction point i was calculated using the following equations:

$$\text{if } d_i \geq D_k \text{ then } \varepsilon_{ik} = D_k + \Delta d_m(\Delta r_{ik}) - d_i \qquad [6]$$

$$\text{if } d_i < D_k \text{ then } \varepsilon_{ik} = d_i - \left(D_k - \Delta d_m(\Delta r_{ik})\right) \qquad [7]$$

$$\varepsilon_i = \sum (\sigma_k + \varepsilon_{ik})\lambda_{ik}\,, \qquad [8]$$

where σ_k is the uncertainty of the observed point k. In the last equation, negative ε_{ik} terms are omitted. This may happen in places with very steep bottom topography.

RESULTS

Function $\Delta d_m(\Delta r)$

Empirical Δd_m values and the fitted functions $\Delta d_m(\Delta r)$ were calculated as described under "peat depth statistics" above for all the mires separately and for the combined dataset of all the mires. Lag size of 5 m and confidence level of 95% (2σ) were used. The problem of solving the fitted parameters for the exponential function (Equation 3) becomes ill-posed when the function approaches a straight line, i.e. at large values of parameter a, where parameters w and a are highly sensitive to even small changes in the data. Thus, the exponential function should not be used for cases where a linear function (Equation 4) fits the data best. In this study, the exponential function was found suitable for all datasets except Kakkurisuo, Heinäsuo1 and Heinäsuo2, where the linear function was applied.

The following sections consider results for each mire separately. Figures 12 and 13 show the empirical values of Δd_m *vs* distance as well as the fitted functions for each dataset for the separation distance range [0, 140] m. The Δd_m(20m) and Δd_m(50m) values, parameters D_0, w and a of the fitted exponential function $\Delta d_m(\Delta r)$ and parameters D_0 and k of the fitted linear function for each dataset are given in Table 2.

Heinäsuo: The linear function was used to fit datasets 1 and 2, while the exponential function was more suitable for the combined dataset 1+2. The Δd_m(20m) values for all the datasets were similar (55−65 cm). The Δd_m(50m) value of dataset 1 is 108 cm and that of dataset 2 is 135 cm. Thus, the Δd_m(50m) value of the combined dataset would be expected to be between these values. However, it is obviously dominated by dataset 2, and even slightly

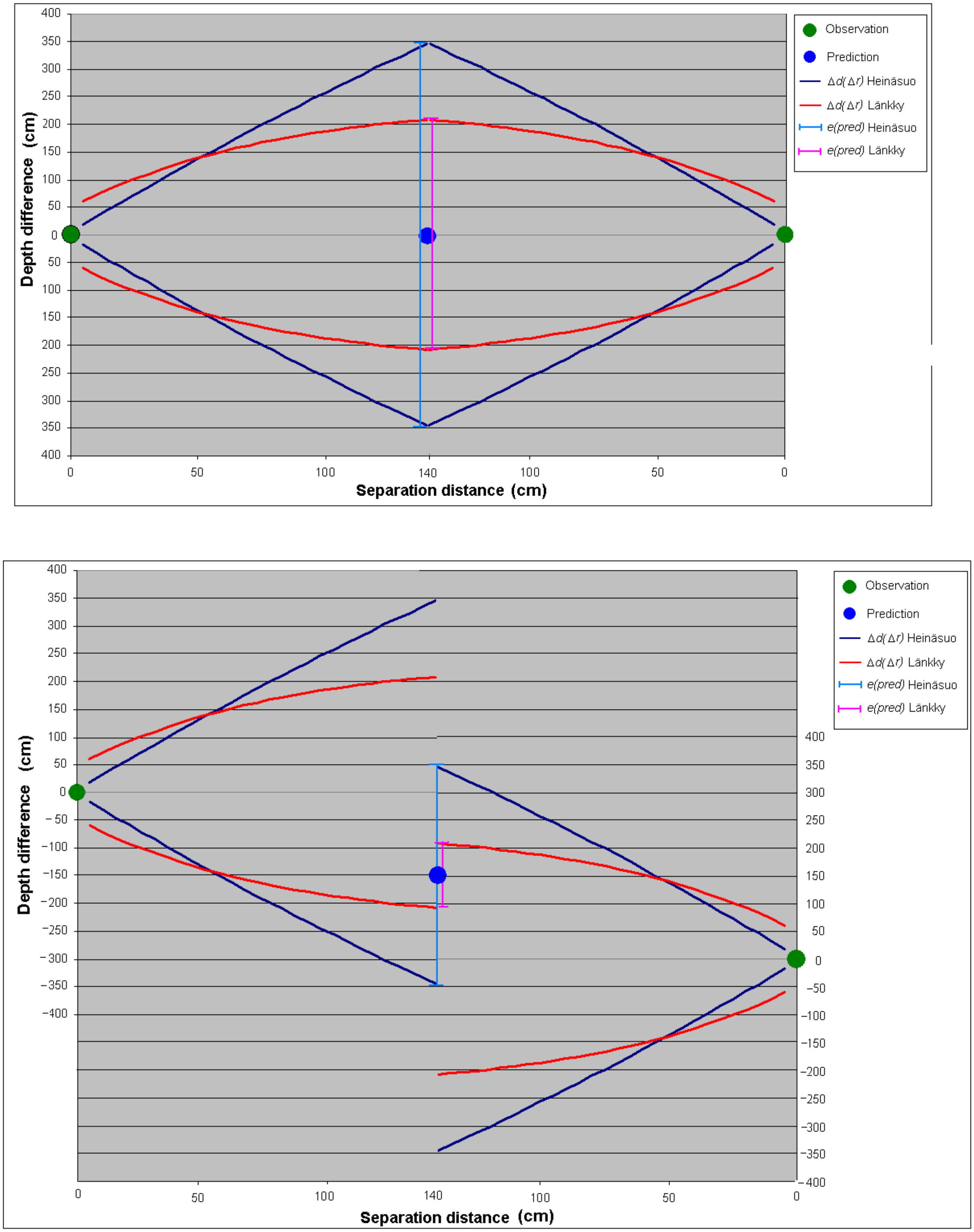

Figure 11. An example of how the uncertainty of the peat thickness prediction between two observations can be defined in cases where there are two observations representing (a) the same depth (upper diagram) and (b) different depths (lower diagram). Two different $\Delta d_m(\Delta r)$ functions were used, one characteristic for Heinäsuo and the other characteristic for Länkkyjärvenneva (abbreviated to Länkky in legend). Parameter $e(pred)$ refers to prediction error and $\Delta d_m(\Delta r)$ to the expected maximum variation of peat thickness at separation distance Δr.

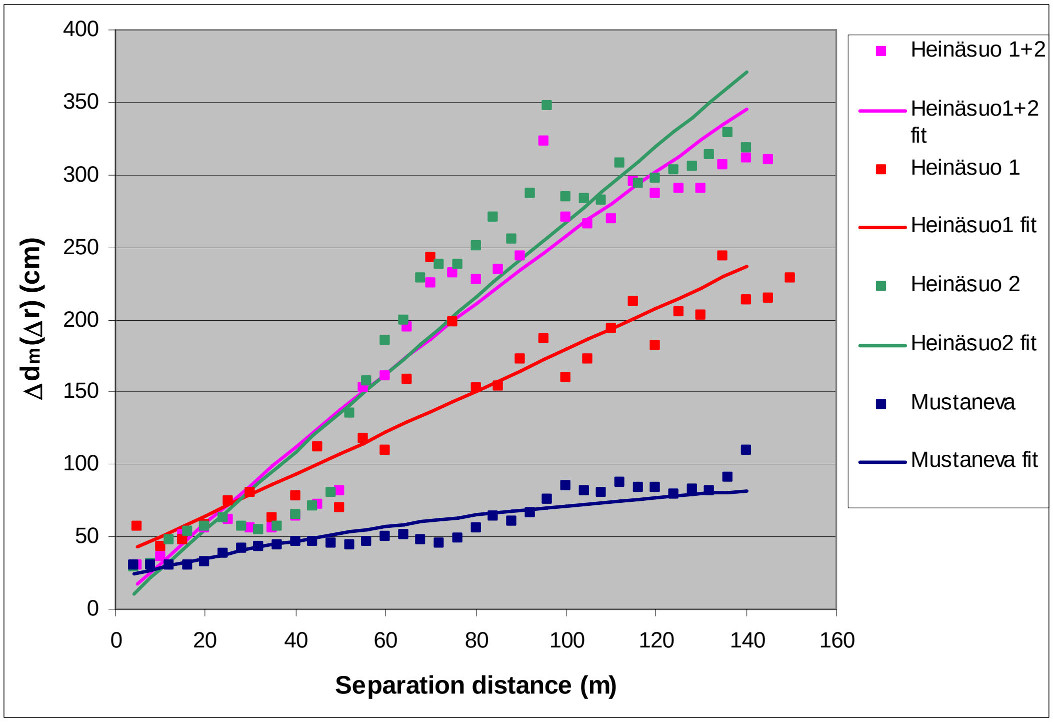

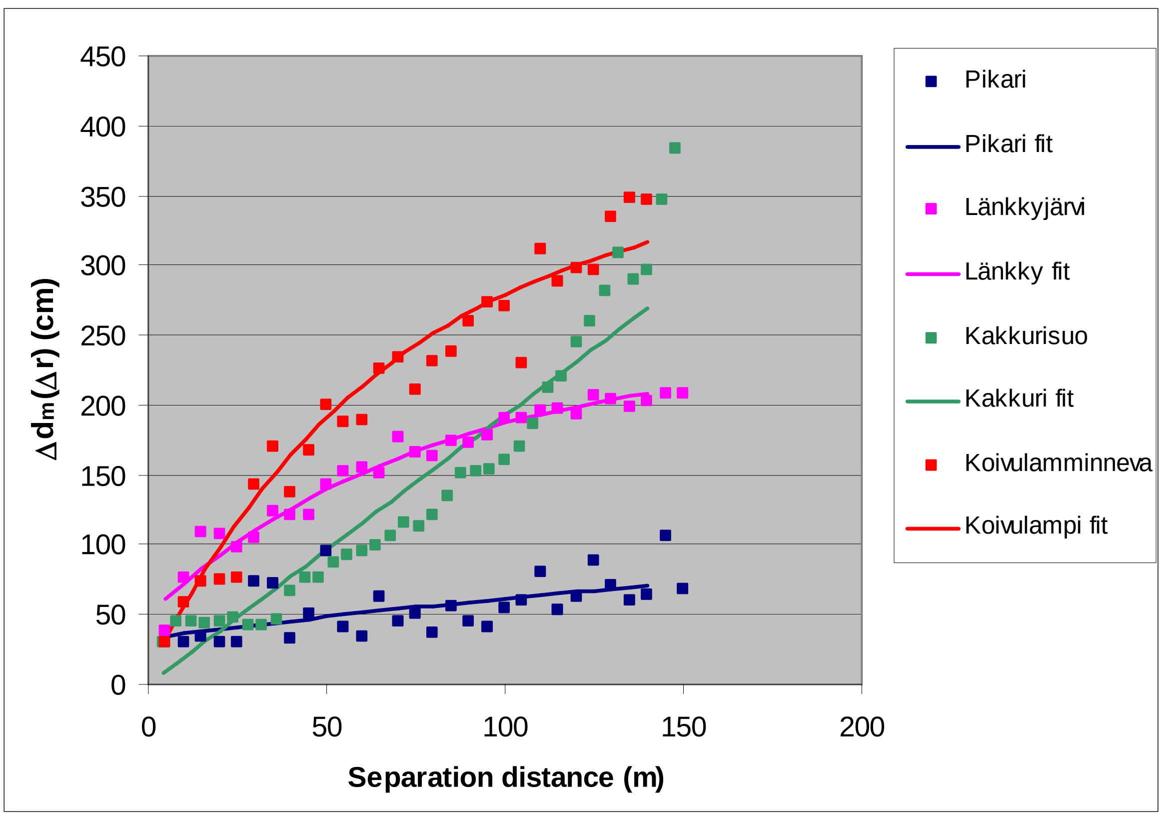

Figure 12. Plot of the expected maximum variation of peat thickness *vs* separation distance for the sample mires, with 2σ confidence, for the separation distance range [0,140] m. An exponential $\Delta d_m(\Delta r)$ function is fitted to all sets of Δd_m values except for Kakkurisuo, Heinäsuo 1 and Heinäsuo 2, where a linear function was applied. Figure (a) (upper diagram) shows plots for Heinäsuo and Mustaneva, (b) (lower diagram) for Pikarineva, Länkkyjärvenneva, Kakkurisuo and Koivulamminneva.

1

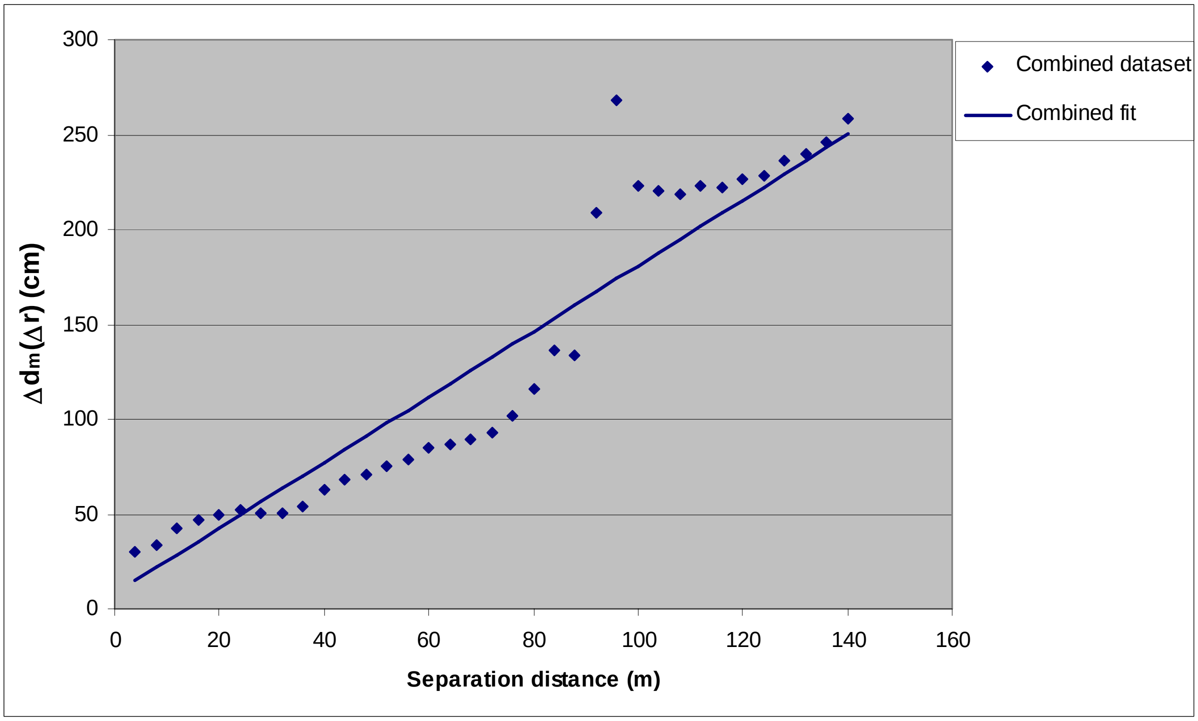

Figure 13. Plot of the expected maximum variation of peat thickness *vs* separation distance for the sample mires, with 2σ confidence, for the separation distance range [0,140] m. Combined dataset with linear function fitted (compare Figure 12).

Table 2. Summary of the results for the different datasets. Values Δd_m(20m) and Δd_m(50m) are the expected maximum depth difference for distance of 20 m and 50 m, respectively, D_0, w, a and k are the parameters of the function fitted to empirical $\Delta d_m(\Delta r)$ values (see Section 2.1 and Equations 1 and 2 for details).

Dataset	**Δd_m(20m) / (cm)**	**Δd_m(50m) / (cm)**	***D_0 / cm***	***w / cm***	***a / cm***	***k***
Heinäsuo1	65	108	36			1.44
Heinäsuo2	55	135				2.75
Heinäsuo1+2	59	137	4	1343	478	
Koivulamminneva	98	191	10	354	70	
Pikarineva	39	48	33	101	304	
Länkkyjärvenneva	92	139	49	191	78	
Kakkurisuo	39	96				1.93
Mustaneva	35	52	21	82	104	
Combined dataset	43	94	8			1.75

larger than that due to the different form of the fitted function. The difference (1 %) is, however, of no importance.

Koivulamminneva: The statistical parameters of Koivulamminneva peat depth are quite similar to those of Heinäsuo (Table 1), but the exponential function $\Delta d_m(\Delta r)$ is different, giving values Δd_m(20m) = 98 cm and Δd_m(50m) = 191 cm, which are larger than those of any other sample mire.

Pikarineva: Pikarineva is the shallowest of the test mire areas with mean depth of about 130 cm, which is close to the mean depth of all measured Finnish peatlands. The variation of the depth with distance is moderate with Δd_m(20m) = 39 cm and Δd_m(50m) = 48 cm, these being among the of the lowest for the sample mires.

Länkkyjärvenneva: Länkkyjärvenneva has similar minimum, maximum and mean merasured peat depths as Heinäsuo, but the standard deviation of the peat depth is smaller, corresponding to a flatter area (Table 1). The value of Δd_m(20m) = 92 cm and of Δd_m(50m) = 139 cm.

Kakkurisuo: Kakkurisuo represents a relatively deep peatland with mean peat thickness close to 3 m. The value of Δd_m(20m) = 39 cm and of Δd_m(50m) = 96 cm.

Mustaneva: The mean depth of Mustaneva is the largest of all the sampled peatlands, 480 cm, but the area is very flat, having a maximum variation in depth of 40 cm for the range of 70 m. The value of Δd_m(20m) = 35 cm and of Δd_m(50m) = 52 cm, these values being among the smallest in the sampled peatlands.

The magnitudes of the Δd_m(20m) values calculated in this study indicate that the dominating part of the uncertainty in field measurements of mire depths is the positioning error, which is 20 m for a typical hand-held GPS (Nyyssönen, pers. comm.). According to the data shown in Figure 13, the error of the observations, for a positioning error of 20 m, is less than 43 cm with 95% confidence. If no mire-specific statistical information is available, the value 43 cm should be used; but it is highly recommended that Δd_m is defined separately for each mire studied in order to obtain the mire-specific, possibly smaller or greater, observational uncertainty. The bottom topography of mires differs significantly; in our sample set Δd_m(20m) is in the range 35−98 cm.

Peat depth model

To show how the function $\Delta d_m(\Delta r)$ affects the uncertainty of the peat depth prediction, exponential functions were fitted to the empirical Δd_m data for Heinäsuo and Länkkyjärvenneva to compute the peat depth model for Heinäsuo. The differences in the depth statistics of Heinäsuo and Länkkyjärvenneva can be seen in Figures 12a and 12b. The Heinäsuo function $\Delta d_m(\Delta r)$ represents a mire where there are moderate depth differences at small separation distances, but the depth differences increase quickly as distances become larger. The Länkkyjärvenneva function $\Delta d_m(\Delta r)$ represents a mire where there are significant depth differences even at small separation distances, but the increase in depth difference towards larger distances is moderate. The uncertainty maps of depth predictions obtained using the functions $\Delta d_m(\Delta r)$ fitted to Heinäsuo and Länkkyjärvenneva data are shown in Figures 14a and 14b, respectively. The prediction uncertainties for the Länkkyjärvenneva-type $\Delta d_m(\Delta r)$ are larger near the observation points than they are for the Heinäsuo-type $\Delta d_m(\Delta r)$ because the observational uncertainty is larger. Far from the observation points, the uncertainty is similar in both cases. It is also evident that the prediction uncertainty is inversely proportional to the depth gradient. Figure 14c shows the predicted depth values and Figure 14d the dataset used for computing the model. The boundary of the modelled region is the mire outline, which is defined by geologists and represents the boundary outside which the peat is less than 30 cm thick. The outline is defined from remote sensing images and complementary field observations and thus is not accurate in all places. For the modelling procedure, it is represented as a set of points of depth 30 cm.

The prediction uncertainty is needed for various purposes in peat research: it gives the uncertainty of predicted depth at any location on the mire; it provides information on how dense the observation grid should be to produce a required accuracy; and it can be used to define the optimal observation grid spacing. As an example, a test was carried out of the way in which the accuracy of the depth models is affected by changing the observing method from the traditional main transect and cross transect approach (with distances of 50 m between points and 200 m between lines) to a square grid with 100 m between points (Laatikainen, 2010). The test involved generating simulated observation points according to both methods and computing the volume of the uncertainty values in the observed area. Results show that, although the depth profiles on the main and cross transect lines become more general (according to the values Δd_m(20m) and Δd_m(50m)), a 20 % decrease in the global uncertainty is achieved by carrying out observations with the new square grid method.

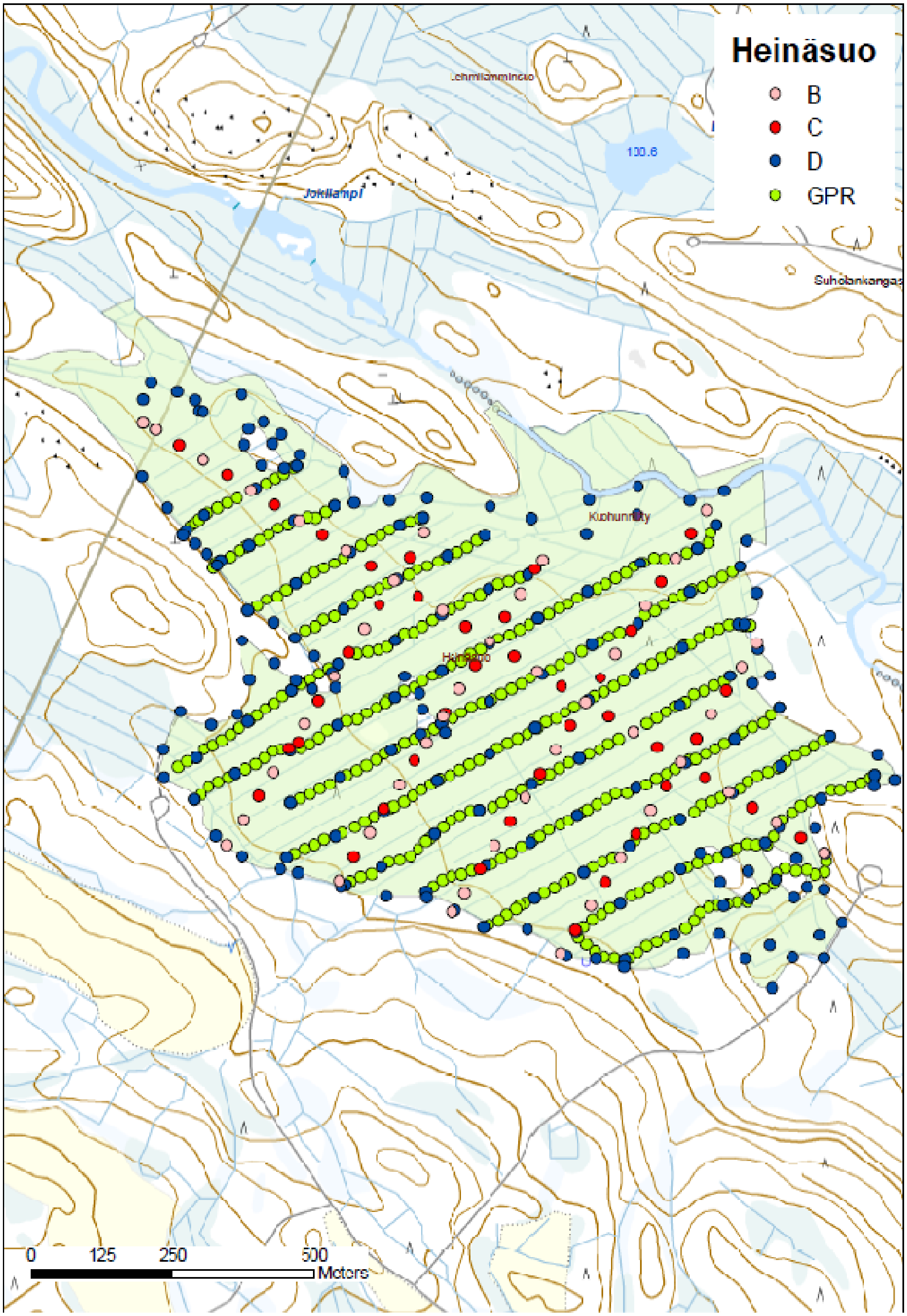

Figure 14. Dataset used to compute the model of Heinäsuo peat thickness using two different types of $\Delta d_m(\Delta r)$ functions to define the prediction uncertainty: one characteristic for Heinäsuo and the other characteristic for Länkkyjärvenneva (see Figure 11). B, C and D points are corings, and GPR points ground penetrating radar measurement interpretations.

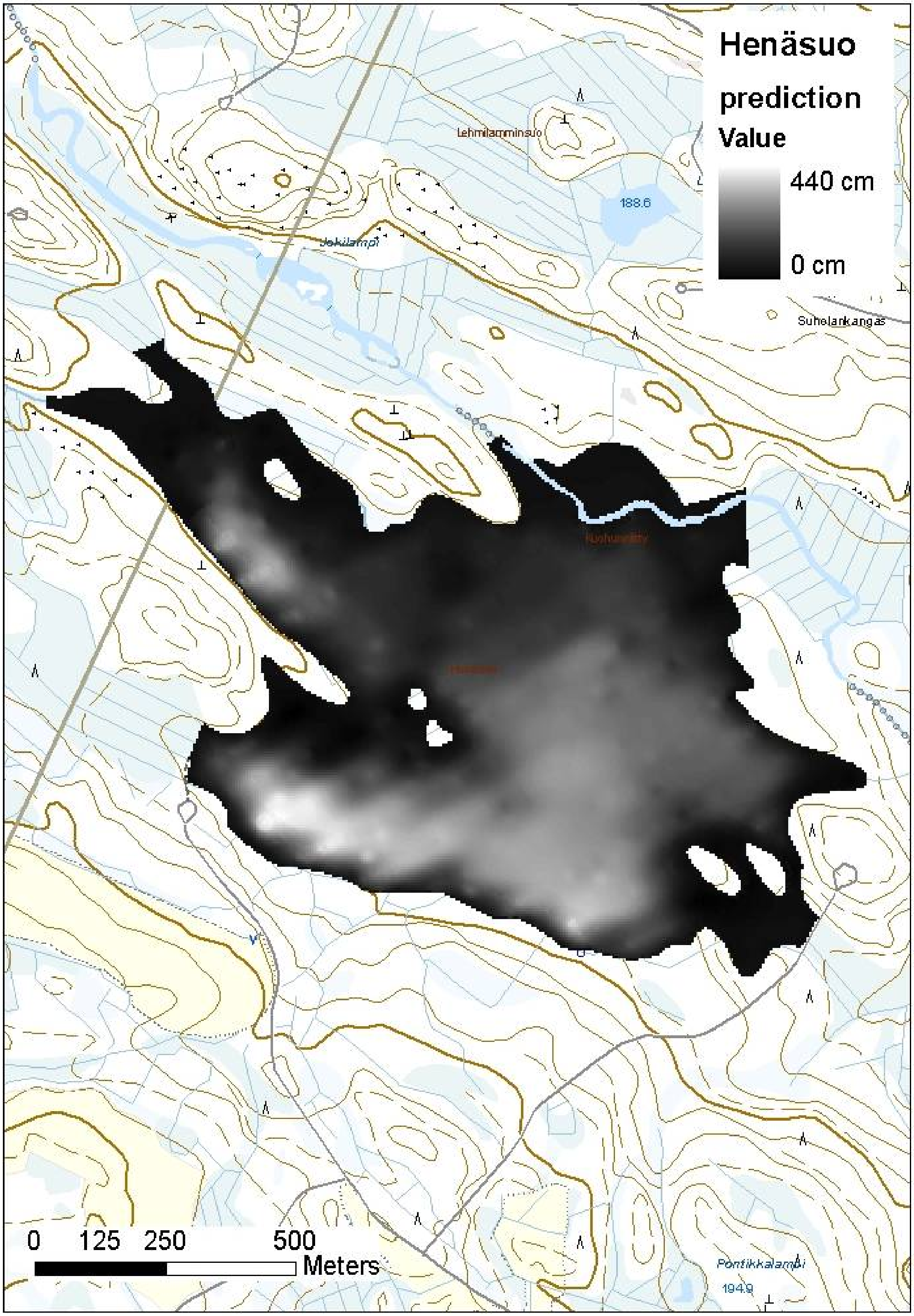

Figure 15. Results of modelling Heinäsuo peat thickness using two different types of $\Delta d_m(\Delta r)$ functions to define the prediction uncertainty: one characteristic for Heinäsuo and the other characteristic for Länkkyjärvenneva (see Figure 11). This Figure shows the peat thickness model. Increasing whiteness represents increasing peat thickness.

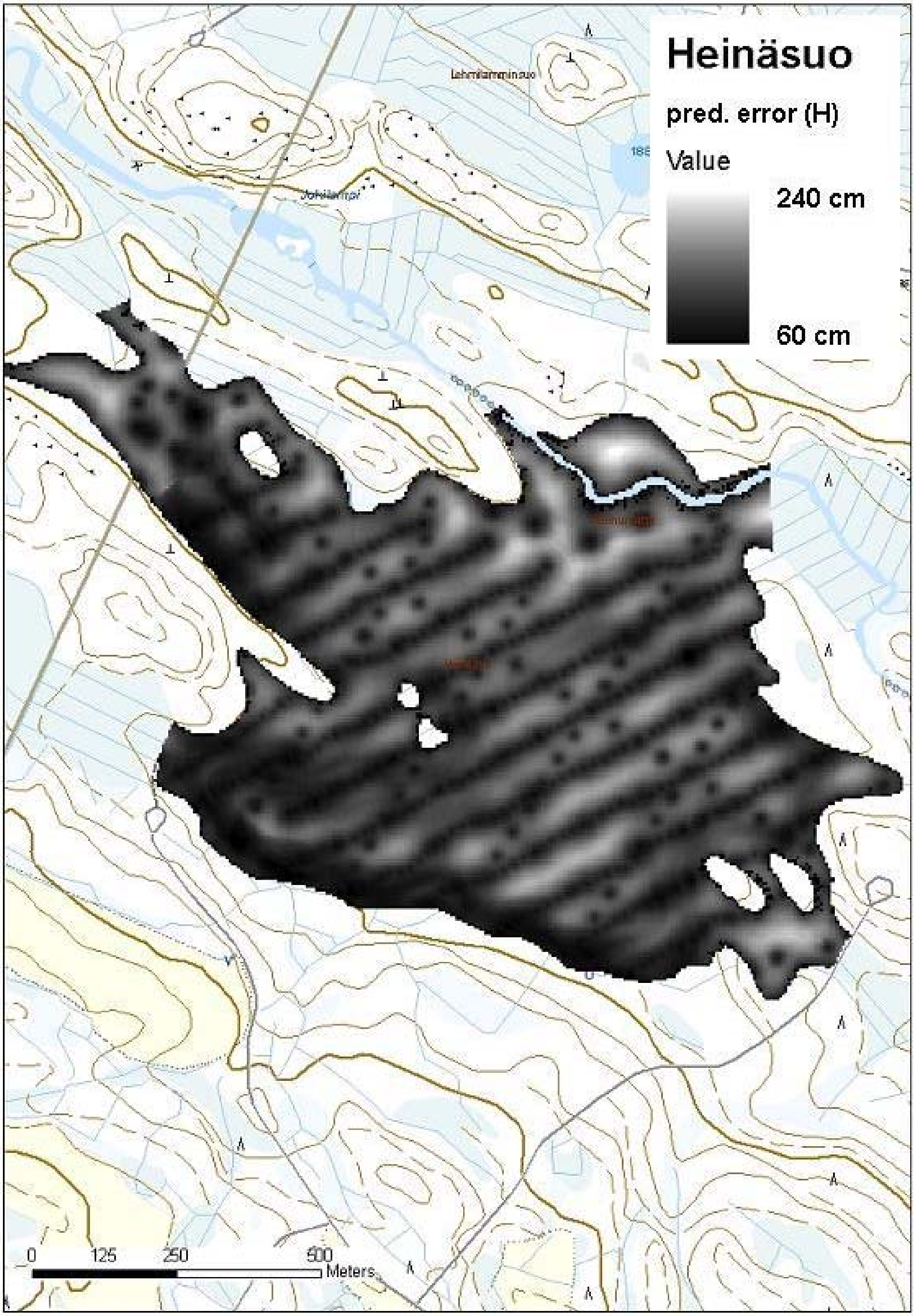

Figure 16. Results of modelling Heinäsuo peat thickness using two different types of $\Delta d_m(\Delta r)$ functions to define the prediction uncertainty: one characteristic for Heinäsuo and the other characteristic for Länkkyjärvenneva (see Figure 11). This Figure shows the uncertainty of the model using parameters characteristic for Heinäsuo (D_0, w, a) = (4, 1343, 478). Increasing whiteness represents increasing prediction uncertainty.

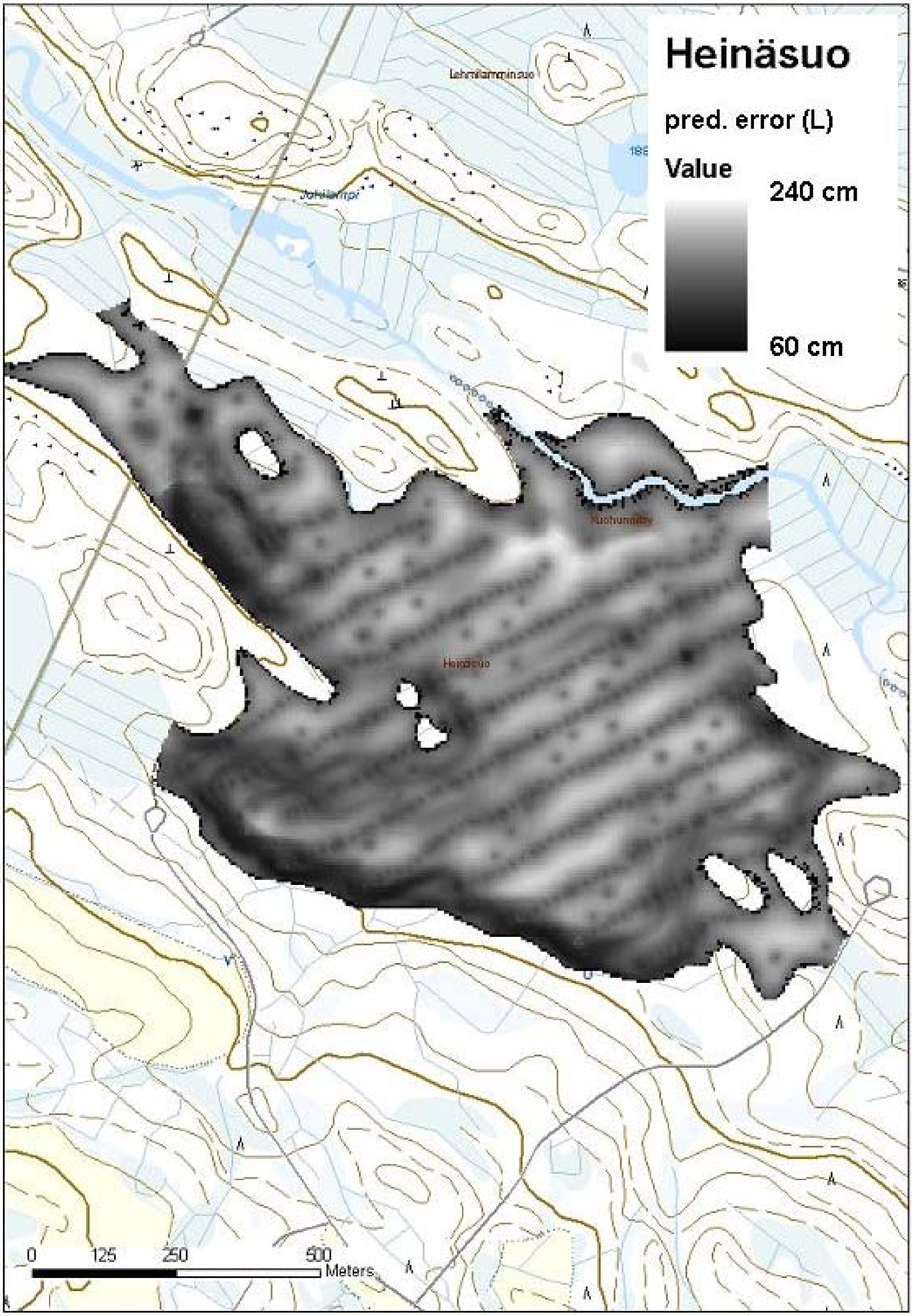

Figure 17. Results of modelling peat thickness at Heinäsuo using two different types of $\Delta d_m(\Delta r)$ functions to define the prediction uncertainty: one characteristic for Heinäsuo and the other characteristic for Länkkyjärvenneva (see Figure 11). This Figure shows the uncertainty of the model using parameters characteristic for Länkkyjärvenneva (D_0, w, a) = (49, 191, 78). Increasing whiteness represents increasing prediction uncertainty.

DISCUSSION

In this article, a statistical approach has been taken to the problem of defining quantitatively the uncertainty of peat thickness measurements and models. The quantity $\Delta d_m(\Delta r)$ (expected maximum variation in peat thickness) was adopted to represent the depth difference below which 95 % of the measured depth differences lie at a certain separation distance Δr. The $\Delta d_m(e_p)$ value gives the observational uncertainty due to positioning error e_p directly, and the $\Delta d_m(\Delta r)$ function can be used in peat thickness modelling to define the prediction uncertainty.

Based on this study, the depth statistics differ remarkably between different mires. Thus, a single $\Delta d_m(\Delta r)$ function, representing the mean for Finnish mires, should not be the first choice; mire-specific $\Delta d_m(\Delta r)$ functions should be determined. This is possible if GPR observations are carried out, since dense GPR interpretations can be made at a sufficient number of locations to obtain the $\Delta d_m(\Delta r)$ function.

For further statistical analysis of peat thickness, it will be necessary to collect $\Delta d_m(\Delta r)$ functions for different types of mires in different geological areas. Once a representative sample of $\Delta d_m(\Delta r)$ functions is at hand (the required number of samples depends on the distribution of $\Delta d_m(\Delta r)$ functions, i.e. their parameters), we can investigate whether there are correlations between $\Delta d_m(\Delta r)$ and other statistical or geological properties of mires, and also search for directional dependences of $\Delta d_m(\Delta r)$. At best, we may find certain types of $\Delta d_m(\Delta r)$ functions being typical for certain types of mires or geological areas.

At the moment, however, the only statistical information on peat thickness of Finnish mires is published in this paper, and the $\Delta d_m(\Delta r)$ functions given should be used for evaluating the uncertainty of the peat thickness observations and models. Although small in number (6), the sample mires are mostly located in areas where steep slopes in mire bottom topography can be expected. Therefore, the $\Delta d_m(\Delta r)$ function defined for the entire data set can be assumed not to underestimate the mean $\Delta d_m(\Delta r)$ for Finnish mires.

When using the observational uncertainty and $\Delta d_m(\Delta r)$ to estimate the prediction error of the peat thickness model, it has to be borne in mind that they define the uncertainty of each individual modelled point but do not directly provide information on the uncertainty of the volume of the peatland. This is because the observation errors are mostly random, and have a destructive effect when integrated over the mire area. Thus, the uncertainty of the volume should be considerably lower than the integrated uncertainty, and depends on the modelling method. One purpose of future studies is to define a realistic uncertainty for the estimated peatland volume.

ACKNOWLEDGEMENTS

I thank Jukka Leino, Matti Laatikainen, Miikka Paalijärvi and Timo Suomi for providing data, and Jukka Turunen and the two anonymous referees for constructive comments. I also thank the K.H. Renlund foundation for funding the work.

REFERENCES

Bárdossy, G. & Fodor, J. (2001) Traditional and new ways to handle uncertainty in geology. *Natural Resources Research*, 10(3), 179–187.

Gustavsson, N. (2010) *Geologisen paikkatiedon epävarmuus* (*The Uncertainty of Geographic Information*). Report TA/2010/7, GTK (Geological Survey of Finland), Espoo, Finland, 145 pp. (in Finnish).

Laatikainen, M. (2011) Turvekartoituksen kenttätutkimusmenetelmän kehittäminen (Development of peatland field survey research method). In: Laatikainen, M., Leino, J., Lerssi, J., Torppa, J. & Turunen, J. (eds.) *Turvetutkimuksen menetelmäkehitystarkastelu* (*A New Approach for Peat Inventory Methods*), Turvetutkimusraportti (Peat Rresearch Review) 414, GTK, Kuopio, Finland (in Finnish).

Leino, J. (2011) Maatutkaluotaus turvekartoituksessa (Mapping peat depth with ground penetrating radar). In: Laatikainen, M., Leino, J., Lerssi, J., Torppa, J. & Turunen, J. (eds.) *Turvetutkimuksen menetelmäkehitystarkastelu* (*A New Approach for Peat Inventory Methods*), Turvetutkimusraportti (Peat Research Review) 414, GTK, Kuopio, Finland (in Finnish).

Torppa, J., Turunen, J. & Lerssi, J. (2011) Turpeen syvyysmallinnus (Peat depth modelling). In: Laatikainen, M., Leino, J., Lerssi, J., Torppa, J. & Turunen, J. (eds.) *Turvetutkimuksen menetelmäkehitystarkastelu* (*A New Approach for Peat Inventory Methods*), Turvetutkimusraportti (Peat Research Review) 414, GTK, Kuopio, Finland (in Finnish).

Submitted 03 Dec 2010, revision 16 May 2011
Editor: R.S. Clymo

Author for correspondence:
Dr Johanna Torppa, Geological Survey of Finland, Eastern Finland Office, Neulaniementie 5, 70211 Kuopio, Finland. Tel: +358 20 55011; Fax: +358 20 55013; e-mail: johanna.torppa@gtk.fi